An Improved Imperialist Competitive Algorithm to Solve the Selected Harmonic Elimination Pulse-Width Modulation in Multilevel Converters

Zheng Gong [1] , **Qi Cui** [1], **Xi Zheng** [1], **Peng Dai** [1,*] **and Rongwu Zhu** [2]

[1] Jiangsu Province Laboratory of Mining Electric and Automation, China University of Mining and Technology, Xuzhou 221008, China; gzcumt@163.com (Z.G.); kuangdarencuiqi@sina.com (Q.C.); 15262017302@163.com (X.Z.)

[2] Chair of Power Electronics, Chritian-Albrechts- University of Kiel, 24118 Kiel, Germany; rzh@tf.uni-kiel.de

* Correspondence: 13329285666@189.cn; Tel.: +86-150-0521-5026

check for updates

Abstract: The traditional intelligent algorithms for the selected harmonic elimination pulse-width modulation (SHEPWM) of multilevel converters provide low convergent rate and low accuracy of solutions when solving quarter-wave symmetry nonlinear equations. To obviate this problem and obtain a better modulating performance, an improved imperialist competition algorithm is proposed. The proposed algorithm enhances the global search ability by using moving imperialists. Also, a novel type of particles, named independent countries, are proposed to help the algorithm jump out of the local optimum. These independent countries change their positions using swarm intelligence. Compared with the existing particle swarm algorithm and genetic algorithm, the proposed algorithm has significant advantages by improving the accuracy of solutions and the rate of convergence. Finally, the correctness and effectiveness of the proposed algorithm are verified and evaluated by simulation and experimental results.

Keywords: multilevel converter; selected harmonic elimination; genetic algorithm; imperialist competitive algorithm

---

1. Introduction

Multilevel converters have been widely applied in high-voltage and high-power applications because of their advantages of effectively improving the quality of output voltage waveform, large output capacity, and high inverting efficiency [1,2]. They have been employed for many industrial applications, such as electrical motor drives [3], energy storage systems [4], and renewable power generators [5]. Moreover, they are also considered as active power filters [6,7] to satisfy the urgent grid-friendly requirements. There are several methods, such as sinusoidal pulse-width modulation (SPWM), space vector pulse-width modulation (SVPWM), and selective harmonic elimination pulse-width modulation (SHEPWM), that can be applied to multilevel converters. As shown in Table 1, compared with the other two methods, the most attractive advantage of the SHEPWM is that the low-order harmonics can be controlled. In addition, SHEPWM also keeps the advantages of a wide modulation index and a high utilization of DC voltage [4]. It was also verified that SHEPWM could be implemented with the objective of minimizing total harmonic distortion (THD) [8].

The key challenge for the SHEPWM technique is to solve nonlinear equations containing trigonometric functions to obtain the right switching angles. A lot of contributions have been made to address this issue in recent years. In a study [9], the Walsh functions are employed to transform nonlinear equations into a series of linear algebraic equations, which can be easily calculated online, providing various sets of solutions. Nevertheless, the transitions between the Walsh series and the

Fourier series requires an effective algorithm, and the high-accuracy requirement may cause an extra heavy computation [10]. In reference [11], high-order equations are transferred to simple trigonometric polynomials, and the calculation mass is greatly reduced by employing the resultant theory. However, the increase of the switching angles enlarges the polynomial order and makes it very difficult to be implemented; also, if there are several DC sources, the expression of the resultant polynomials becomes more complicated [12]. The Homotopy algorithm is adopted to solve the equations in other studies [13,14]. It features a rapid convergence and can be extended to the high-level converters without any extra analytical calculations. Moreover, only one set of solutions can be obtained by this algorithm. In references [15,16], the Newton–Raphson algorithm is applied to solve nonlinear equations. This algorithm keeps a high accuracy and a low computation burden, but its implementation strongly relies on the accuracy of the initial values. If the predictions of these initial values are not around the right solution, the solving process would plunge into local optima. Meanwhile, there is still only one sets of solutions that can be determined in each solving instant. A novel Groebner–Bases-based method is presented in reference [17], which transforms the nonlinear equations into an equivalent canonical system and improves the accuracy of the solutions. However, the transformation becomes very complex when the order of the equations is high, making this method more complicated than the previous methods.

Table 1. Comparison of sinusoidal pulse-width modulation (SPWM), space vector pulse-width modulation (SVPWM), and selected harmonic elimination pulse-width modulation (SHEPWM).

Modulation Type	SPWM	SVPWM	SHEPWM
DC voltage utilization	0~0.866	0~1	0~1.12
Switching frequency	Medium	High	Low
Complexity of strategy	Low	High	High
Implementation approach	Online	Online	Offline

On the basis of the review above, it is seen that the aforementioned solving methods for the SHEPWM are commonly complex and not available for all sets of solutions. Actually, the problem of solving the SHEPWM can be reformulated into a constraint optimization problem, and many intelligent algorithms can also be adopted to solve this problem [18–22]. They not only can find all solutions, but also can be expediently applied to the multilevel converters with equal or non-equal DC voltage sources.

The genetic algorithm (GA) has been used in SHEPWM for many years. It is an algorithm which was inspired by natural biological evolution. This approach employs selection, crossover, and mutation operators and starts by randomly generating the individuals of a population. The individuals represent the properties of a solution and can be mutated and crossover to evolve toward better solutions. As we can see, the GA is simple and easy to understand but, as the required switching angles increase, the distortion of the output voltage gets worse. A new GA algorithm in reference [18] divided a population into several independent populations whose individuals can migrate from one to another. This improved algorithm, named multi-population genetic algorithm (MGA), can settle the problem of precociousness efficiently, but the accuracy of solutions still demands improvement. Particle swarm optimization (PSO), a common algorithm, simulates the predation behaviour of bird flocks and has been proved very efficient in precision and convergent rate compared with GA. Each particle of PSO has personal and global best positions which guide it towards to the optimal solution. The PSO in reference [19] is used to solve a problem that reduces the computation. In reference [20], a constriction factor was introduced, and a method to obtain proper constriction factor and acceleration coefficients was described. The advanced algorithm improves the precociousness problem but still lacks global search ability.

The imperialist competitive algorithm (ICA) is inspired by imperialistic competition and includes two primary categories: imperialists and colonies. The major steps are colonies assimilation and empires' competition. The research presented in references [21,22] has proved the ascendency of the

ICA in rate and speed of convergence. The contribution described in reference [23] is the first attempt to apply the ICA to solve the SHEPWM of power converters. It has been proved that this conventional ICA algorithm can solve nonlinear equations when the dimension of the variable is low. However, the convergent rate decreases, and the accuracy of solutions of the conventional ICA becomes worse with the increasing dimension of multilevel converters. Hence, the solving execution time will be longer, and the modulation accuracy will not be guaranteed.

To improve the ICA-based SHEPWM for multilevel converters, a novel kind of solving method based on the particles named the independent countries is proposed in this paper. The optimized design is conducted from two starting points: one is to increase the diversity and movements of the imperialists, the other is to enhance the ability to jump out of the local optimal. This optimized design is expected to obtain high convergent rates and high accuracy solutions when the converter' dimension increases. In addition, with taking the neutral-point-clamped H-Bridge (NPC/H-Bridge) five-level converter [24] as a typical multilevel converter for the application, sufficient comparative analysis and simulation research regarding various kind of solving methods for the multilevel SHEPWM are carried out to present the characteristics and advantages of the proposed method. Finally, experimental research is also conducted with a downscaled NPC/H-Bridge five-level converter prototype to validate its practical applicability.

The rest of this paper is divided as follows. Section 2 introduces the topology of the NPC/H-Bridge five-level converter and the basic principle for solving the SHEPWM. Section 3 presents the novel intelligent algorithm and compares it to three existing algorithms in detail. Simulation results and best solutions regarding the condition of two switching angles per quarter wave are described and evaluated in Section 4. The experimental results are shown in Section 5, and Section 6 concludes this paper.

2. NPC/H-Bridge Five-Level Converter and SHEPWM Switching Strategy

2.1. NPC/H-Bridge Five-Level Converter

Figure 1 shows the topology of the NPC/H-Bridge five-level converter. As shown, compared to the conventional neutral-point-clamped (NPC) [25], flying capacitor (FC) [26] topologies, this topology needs fewer clamping diodes or capacitors, which reduces the cost and improves the stability of system. Besides, compared to the modular multilevel converters (MMC) [27] cascaded H-Bridge (CHB) [28] topology, the number of DC-side power supplies can be reduced, and then the large number of capacitors or the bulky multiple isolation transformers can be reduced. For the NPC/H-Bridge five-level converter, each phase unit consists of two single-phase three-level NPC-type bridge arms, two DC-side capacitors, and one DC voltage source. In each NPC-type bridge arm, there are four power switching devices (along with the forward diodes) and two clamped power diodes.
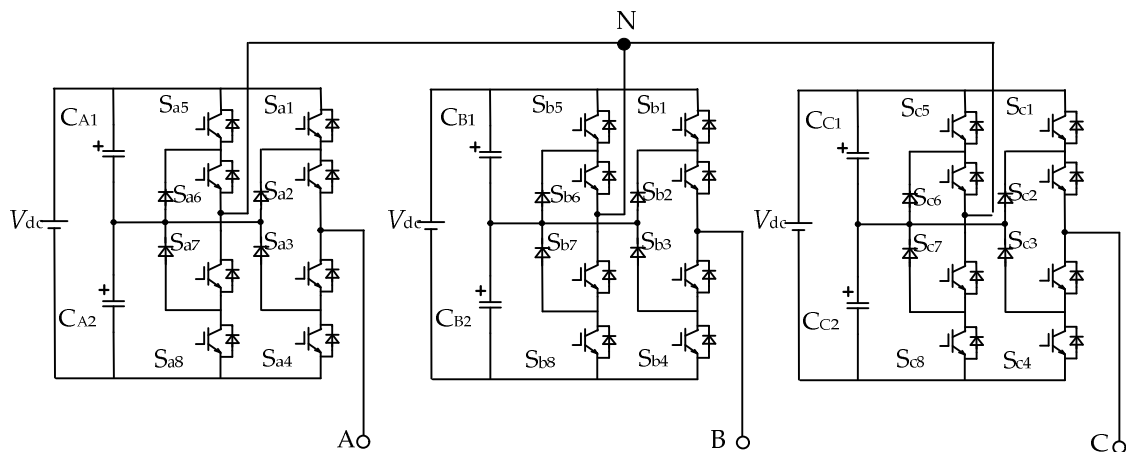

**Figure 1.** Three-phase NPC/H bridge five-level inverter topology.

Taking phase A as an example, it can be seen that the switching devices Sa1–Sa4 cascade the right bridge, while the Sa5–Sa8 cascade the left bridge. Each bridge can generate three voltages, i.e., $+1/2V_{dc}$, 0, and $-1/2V_{dc}$ by different switching angles, so the output voltages of phase A include $+V_{dc}$, $+1/2V_{dc}$, 0, $-1/2V_{dc}$, $-V_{dc}$. Table 2 shows the switching states of the NPC/H bridge five-level inverter. S_{x1}-S_{x8} represent the switching states of IGBTs. V_{XN} is the value of output voltage. In this paper, the switching states 1, 2, 5, 8, and 9 are chose to synthesize the output waveforms.

Table 2. Switching states of the NPC/H bridge five-level inverter.

Number	$S_{x1}, S_{x2}, S_{x3}, S_{x4}, S_{x5}, S_{x6}, S_{x7}, S_{x8}$ (x = a, b, c)	V_{XN} (X = A, B, C)
1	11000011	V_{dc}
2	11000110	$V_{dc}/2$
3	11000110	
4	11001100	
5	01100110	0
6	00110011	
7	01101100	$-V_{dc}/2$
8	00110110	
9	00111100	$-V_{dc}$

2.2. Basic Principle for Solving the SHEPWM

Figure 2 shows the output voltage waveforms at the high and low modulation shown in Figure 1. Every quarter-wave of a waveform includes two switching angles. These angles are symmetric to $\pi/2$ in a half period and conform to the so-called quarter-wave symmetry technique [29]. Compared to the half-wave symmetry and asymmetry techniques [15,30], the quarter-wave symmetry technique can simplify nonlinear equations and reduce the computation burden.
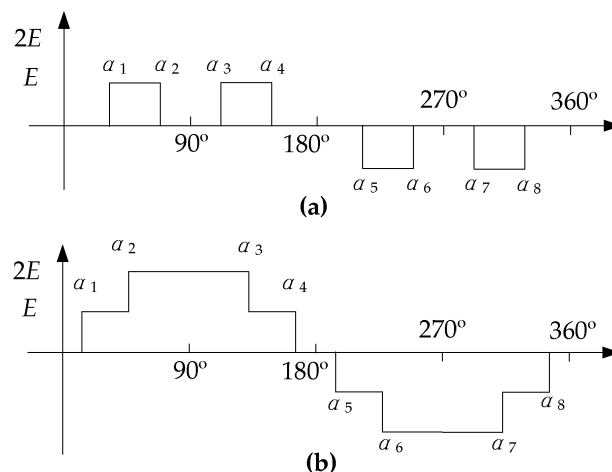
Figure 2. Pulse width modulation (PWM) waveforms definition of two switching angles according to the quarter-wave SHEPWM techniques. (**a**) Waveform at low modulation width; (**b**) waveform at high modulation width.

Equation (1) shows the Fourier series expansion of the full cycle.

$$V(t) = a_0 + \sum_{n=1}^{\infty} (a_n \cos n\omega t + b_n \sin n\omega t) \tag{1}$$

where n = 1, 2, 3 . . .

Because of the characters of quarter-wave symmetry, the DC component a_0 and the cosine component a_n are equal to zero. The sine component is zero when n is even. Equation (1) is simplified as follow:

$$\begin{cases} a_n = 0, \ n = 0, 1, 2, 3 \ldots \\ b_n = \begin{cases} 0, \ n \text{ is even} \\ \frac{4E}{n\pi} \sum\limits_{k=1}^{N} (-1)^{k+1} \cos n\alpha_k \end{cases} \end{cases} \tag{2}$$

Because all triple harmonics are removed in line voltage, only the $6k \pm 1$th harmonic should be eliminated. Equation (3) is the simplified Equation (2):

$$\begin{cases} \frac{2}{\pi} \sum\limits_{k=1}^{N} p_k \cos \alpha_k = M \\ \sum\limits_{k=1}^{N} p_k \cos n\alpha_k = 0 \quad n = 5, 7, 11, \ldots, 6k \pm 1 \end{cases} \tag{3}$$

where p_k indicates the rising or falling edge of the output voltage, which is given by Equation (4):

$$p_k = \begin{cases} 1 & \text{rising edge} \\ -1 & \text{falling edge} \end{cases} \tag{4}$$

According to the waveform of the five-level converter, the polynomial equations can be simplified to Equation (5):

$$\begin{cases} \cos \alpha_1 + \cos \alpha_2 - M\pi/2 = \varepsilon_1 \\ \cos 5\alpha_1 + \cos 5\alpha_2 = \varepsilon_2 \end{cases} \tag{5}$$

$$f(\alpha) = \varepsilon_1{}^2 + \varepsilon_2{}^2 \tag{6}$$

Equation (6) is the cost function of the intelligent algorithm, which is built on Equation (3). Different switching angles can be calculated when the modulation index is changed.

3. The Proposed Improved Imperialist Competitive Method for Multilevel SHEPWM

3.1. Design of the Improved Imperialist Competitive Algorithm

ICA establishes a mathematical model based on imperialistic competition and belongs to the random optimization search methods. ICA generates initial countries (which equal to particles of PSO or chromosomes of GA) within the search space. A number of countries are selected as imperialists according to their fitness, and the remaining countries are randomly allocated to the imperialists as colonies. An imperialist and its colonies constitute an empire. Then, each imperialist assimilates its relative colonies, and the empires compete with each other until only one empire remains or the terminal condition is achieved. The main steps of ICA are as follows:

(1) Generating initial countries. The algorithm randomly generates N_{pop} initial countries within the search space. For a N_{var} dimensional problem, a country is defined according to Equation (7). Then, the first N_{imp} powerless countries are selected as imperialists, according to Equations (8)–(10). Colonies are assigned to each imperialist, according to Equation (11).

$$\text{country} = [d_1, d_2, d_3, \ldots, d_{N_{\text{var}}}] \tag{7}$$

$$\text{cost} = f(\text{country}) = f(d_1, d_2, d_3, \ldots, d_{N_{\text{var}}}) \tag{8}$$

$$C_n = c_n - \max_i \{c_i\} \tag{9}$$

$$p_n = \left| \frac{C_n}{\sum_{i=1}^{N_{imp}} C_i} \right| \tag{10}$$

$$N.C_n = round\{p_n \times N_{col}\} \tag{11}$$

where c_n is the cost of the nth imperialist, and C_n and p_n are its normalized value and power. $N.C_n$ in Equation (11) represents the number of colonies of every imperialist.

(2) Assimilating colonies. Each imperialist improves its colonies by changing their positions. All colonies move toward the imperialist according to Equations (12) and (13):

$$Vector_n = imp^{i-1} - col_n^{i-1} \tag{12}$$

$$col_n^i = col_n^{i-1} + r_4 * \text{rand}(1, N_{\text{var}}). * Vector \tag{13}$$

col_n^i and col_n^{i-1} mean the current and previous positions of the nth colony, and r_4 is the assimilation coefficient. During this process, if the cost of any colony is less than the cost of the relative imperialist, the imperialist position is updated.

(3) Imperialistic competition. The most powerful empire takes possession of the worst colony of the weakest empire by two procedures.

(a) Calculating the total costs of empires.

$$T.C_n = f(imp_n) + \xi \times \frac{\sum_{i=m}^{N.C_n} f(col_m)}{N.C_n} \tag{14}$$

In Equation (14), $T.C_n$ means the total cost of the nth empire, and ξ is a positive number less than 1.

(b) The empire which has the largest $T.C_n$ is regarded as the weakest empire, and its worst colony is captured by other empires, according to Equations (15) and (16):

$$N.T.C_n = T.C_n - \max_i\{T.C_i\} \tag{15}$$

$$R_n = \left| \frac{N.T.C_n}{\sum_{i=1}^{N_{imp}} N.T.C_n} \right| \tag{16}$$

where $T.C_n$ and $N.T.C_n$ indicate the total cost and normalized total cost, respectively. R_n is the probability of the nth empire capturing the worst colony.

(4) Eliminating the worst empire. When an empire loses all its colonies, it is deleted.

(5) Reset colonies' positions. When the total cost of the best empire does not change for a long time, reset all colonies' positions of each empire stochastically.

In this paper, not only the colony countries change positions, but also the imperialists move their positions to improve their performance. Also, a type of particles called independent countries is presented to improve the diversity of ICA, which change positions using swarm intelligence. This new hybrid algorithm consists of both PSO and ICA and, thus, it is called PSOICA algorithm. The implementation steps of the proposed PSOICA algorithm are as follows.

(a) Select the first ($N_{\text{imp}} + 1 \sim N_{\text{imp}} + N_{\text{ind}}$) powerless countries as independent countries according to Equations (7)–(9). N_{ind} is the number of independent countries.

(b) Move imperialists and independent countries in line with the PSO procedures. In this step, imperialists and independent countries may gain better positions. This step enhances the global search ability of the algorithm.

$$imp_n^i = imp_n^{i-1} + V_{imp}^i \tag{17}$$

$$V_{imp}^i = c_1 * r_1 * (best_{imp} - imp_n^{i-1}) \tag{18}$$

Move the imperialists on the basis of Equations (17) and (18); imp_n^i and V_{imp}^i indicate the current position and velocity of the nth imperialist, imp_n^{i-1} means the previous position of the nth imperialist, c_1 is a positive number less than 1, and r_1 is a random number between 0 and 1. If the cost of the current position is less than that of the previous position, update the imperialist, otherwise, keep the previous position.

$$V_n^i = \omega * V_n^{i-1} + c_2 * r_2 * (P_l^{i-1} - ind_n^{i-1}) + c_3 * r_3 * (P_g^{i-1} - ind_n^{i-1}) \tag{19}$$

$$ind_n^i = ind_n^{i-1} + V_n^i \tag{20}$$

Equations (19) and (20) show the movement of independent countries, where P_l and P_g are the personal and global best positions of the nth independent countries, V_n^i is the current velocity, ind_n^i is the current position of the nth independent country, ω is the inertia weight, c_2 and c_3 are acceleration constants, and r_2 and r_3 are random numbers between 0 and 1. If the cost of P_g is better for the imperialist, the imperialist moves to P_g, and vice versa if it is worse.

Figure 3 shows the moving steps of the ICA and the proposed PSOICA.
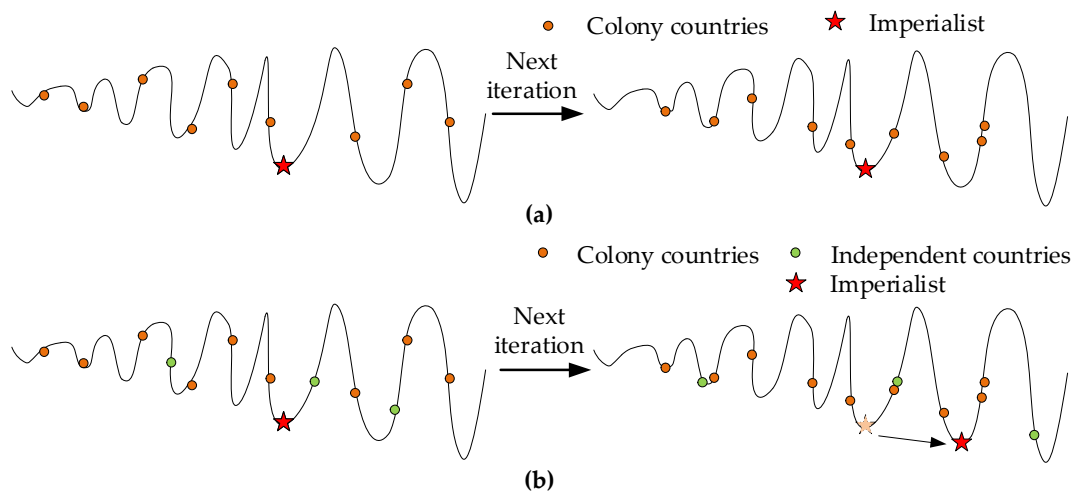
Figure 3. (**a**) Moving steps of the imperialist competitive algorithm (ICA); (**b**) moving steps of the particle swarm optimization (PSO) ICA (PSOICA).

Figure 3a shows the moving steps of the conventional ICA [20,22] when all the colony countries are assimilated by their imperialist, and the imperialist never moves. Figure 3b shows the moving steps of the proposed PSOICA, with all the colony countries moving towards their imperialist. Meanwhile, the imperialist changes its position and then it may move to a better position. The independent countries move to their next positions on the basis of the swarm intelligence, and they may get new better positions or stay in the former positions.

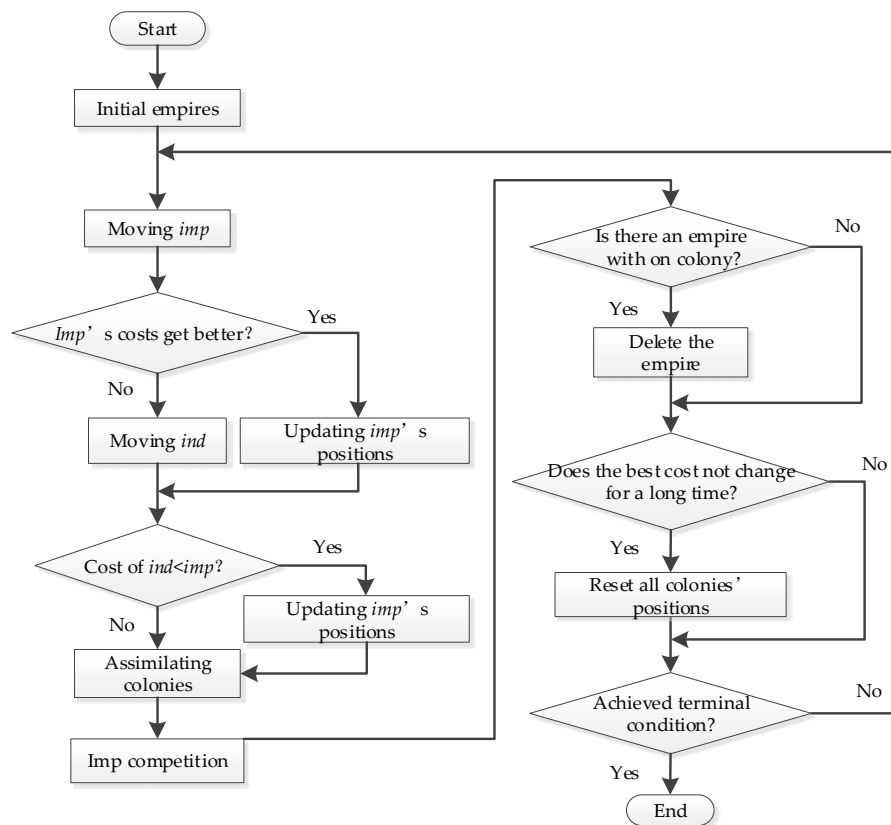Figure 4 shows the flow chart of the proposed PSOICA.

Figure 4. Flow chart of the proposed PSOICA.

3.2. Comparisons with the Existing Methods

To make the comparisons, the MGA [18], PSO [20], ICA [23], and the proposed PSOICA are considered to calculate their cost function. The parameters of three algorithms are set as follows: for MGA, the populations re 10, and each of them has 40 chromosomes; the initial crossover rates are random numbers between 0.7 and 0.9, and the mutation rates are random numbers between 0.2 and 0.35; for PSO, the particles are 400, both the acceleration coefficients are 1.49445, and the inertia weight increases along with iteration from 0.21 to 0.7; for ICA, there are 400 initial countries and 20 imperialists, and c_1, c_2, c_3 are equal to 0.95, 0.5, 0.5, ω is 0.7298, and the assimilation coefficient r_4 is 2.5; for the proposed PSOICA, there are 400 initial countries, 20 imperialists, 20 independent countries, and c_1, c_2, c_3, ω, and r_4 are the same as for ICA.

In Table 3, the efficiency and feasibility of the proposed PSOICA for the optimization of SHEPWM are compared with those of three other algorithms.

Table 3. Comparing the performance of the PSOICA to those of the multi-population genetic algorithm (MGA), PSO, and ICA.

m	Switching Angles		THD%	$f(\alpha)$			
				MGA	PSO	ICA	PSOICA
1.1	6.715	42.72	18.34	2.95×10^{-11}	4.93×10^{-32}	4.93×10^{-32}	4.93×10^{-32}
1	16.33	52.33	19.27	9.80×10^{-11}	4.93×10^{-32}	4.93×10^{-32}	4.93×10^{-32}
0.9	23.99	59.99	26.58	1.02×10^{-11}	4.93×10^{-32}	4.93×10^{-32}	2.77×10^{-32}
0.8	30.65	66.65	35.21	5.06×10^{-17}	0	0	0
0.7	36.7	72.68	43.95	1.08×10^{-8}	0	0	0
0.6	42.3	78.3	52.64	8.53×10^{-10}	1.233×10^{-32}	1.23×10^{-32}	1.11×10^{-31}
0.5	47.61	83.61	60.7	3.62×10^{-11}	4.93×10^{-32}	4.93×10^{-32}	1.97×10^{-31}
0.4	52.71	88.71	65.51	1.64×10^{-11}	4.93×10^{-32}	4.93×10^{-32}	4.93×10^{-32}
0.3	57.69	86.31	88.04	1.01×10^{-6}	3.081×10^{-33}	3.08×10^{-33}	0
0.2	62.5	81.5	128.72	5.04×10^{-8}	1.233×10^{-32}	1.23×10^{-32}	1.77×10^{-30}
0.1	67.26	76.74	205.63	5.12×10^{-8}	7.704×10^{-34}	7.70×10^{-34}	7.70×10^{-34}

It should be noticed that all four algorithms converge successfully, and all the THD under the same modulation index unify, which means that all the algorithms can solve the nonlinear equations efficiently when only two switching angles are included. The cost values show that the PSO, ICA, and the proposed PSOICA are better than the MGA in local search. The cost of the MGA is about 1×10^{-10}, and those of the PSO, ICA, and PSOICA are about 1×10^{-30}.

At low modulation index, if more selected harmonics of output voltage have to be eliminated, the switching angles per quarter wave should be increased. Table 4 shows the results of the four algorithms when we compare the best costs of five computations. Each quarter wave includes four angles.

**Table 4.** Switching angles and costs at 0.2 modulation index.

Algorithms	$\alpha 1$	$\alpha 2$	$\alpha 3$	$\alpha 4$	$f(\alpha)$
MGA	51.219	57.315	73.357	84.342	0.001912
PSO	50.893	57.74	72.439	85.149	1.76×10^{-31}
ICA	50.894	57.74	72.439	85.148	2.38×10^{-10}
PSOICA	50.893	57.74	72.439	85.149	1.68×10^{-30}

As can be seen, the switching angles of the MGA deteriorated, and the cost are bigger than 1×10^{-5}. Figure 5a shows the simulation results of the MGA. The output voltage distortion could not be ignored. In contrast, the costs of the PSO, ICA, and the proposed PSOICA are much smaller than 1×10^{-5}. However, with the increasing switching angles, the accuracy of the solution could worsen. Comparing Table 3 with Table 4, the accuracy of the solutions calculated by the ICA or the MGA decreases rapidly with the increasing switching angles, while the costs of the PSO and the PSOICA have no significant changes. Hence, the advantages of the PSO and PSOICA algorithms in local searching ability are further confirmed. Figure 5b,c exhibits the phase voltages and corresponding spectra.

As shown in Figure 5, when the switching angles increase to 4, the MGA cannot eliminate the 5th harmonic completely, and the phase voltage distortion raises to 9.2%. In contrast to the MGA, the 5th, 7th, and 11th harmonics are eliminated by the PSO, ICA, and proposed PSOICA. At the same time, the phase voltages also meet the desired values.

The results show that the dimension of the variables has a large influence on the precision of solutions. In Figure 6, the phase voltage distortion rates and the THDs of the four algorithms are plotted with respect to the modulation degree in the situation of four switching angles per quarter wave.

As we can see, the phase voltage distortion rates (PVDR) of the MGA even reach 40%, which is quite higher than the those of PSO, conventional ICA, and proposed PSOICA, whose PVDR ar on the average, 1%. That means that the MGA performs worse in high variable optimization problems. In contrast, the PSO, conventional ICA, and proposed PSOICA can output the desired voltage effectively and eliminate the selective harmonics. However, there is a big difference between these three algorithms. They have different THD of phase voltages. For PSO and ICA, the THDs decrease with modulation increase but, in some situations, the THDs get higher. For the proposed PSOICA, THD is an obvious attenuation curve. This is because in low modulation index, the nonlinear equations with the four switching angles have three different solutions, and each of them has different THDs. The PSOICA finds the best optimal solution that has the lowest THD each time. However, the ICA and PSO frequently result in suboptimal solutions, with higher THDs due to the searching limitation.
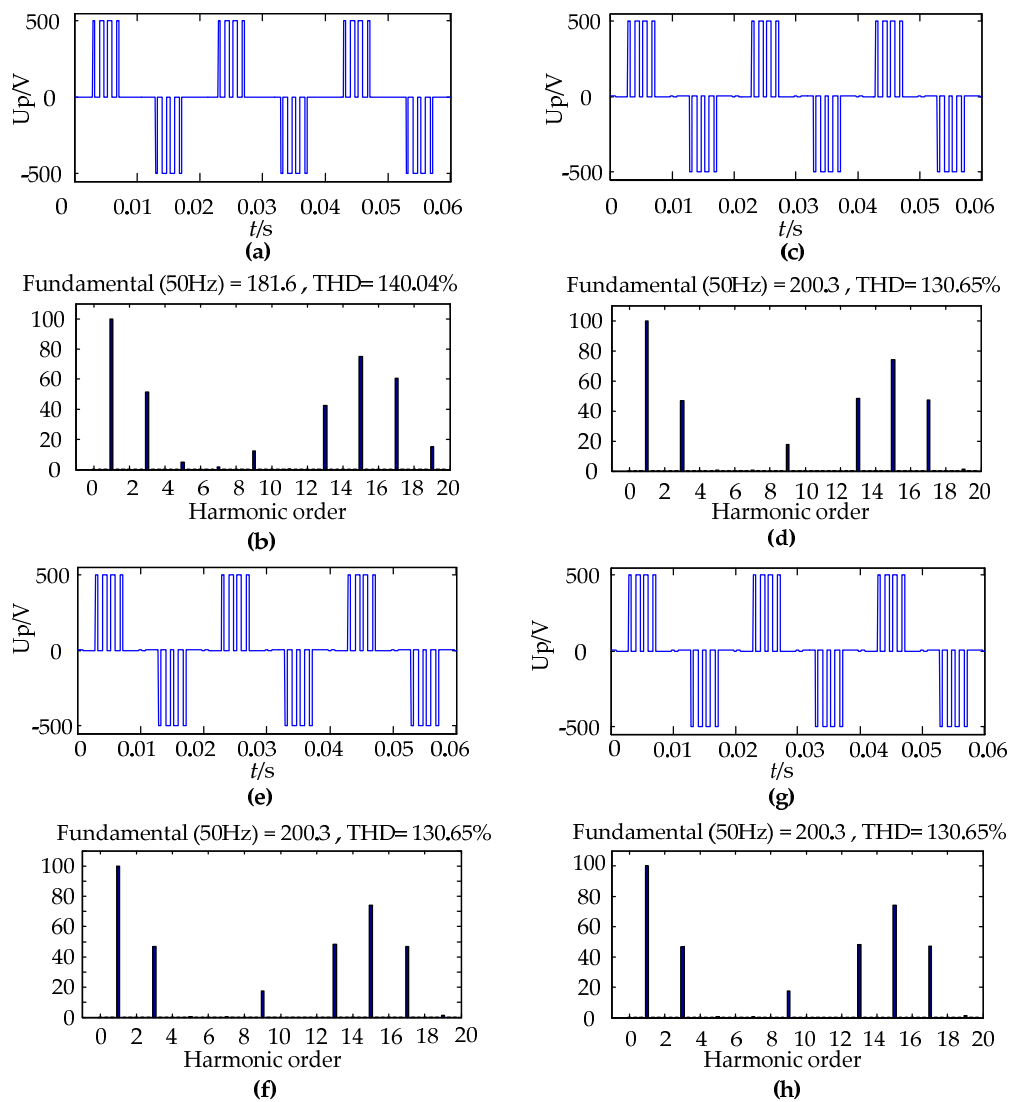
Figure 5. Waveforms of phase voltage and spectrum analysis of four algorithms: (**a**,**b**) MGA; (**c**,**d**) PSO; (**e**,**f**) ICA; (**g**,**h**) the proposed PSOICA. THD: total harmonic distortion.
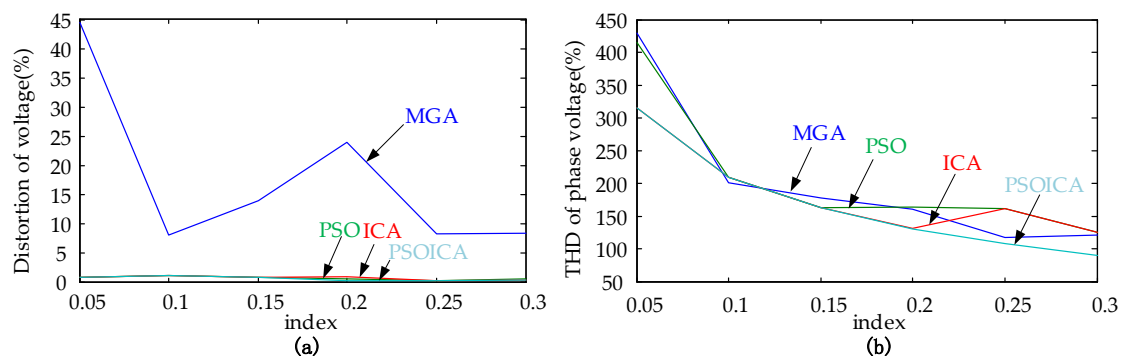
Figure 6. Characteristic analysis: (**a**) voltage distortion rate; (**b**) THDs.

Therefore, we come to the conclusion that, when the dimension of the cost function increases, the local search ability of the MGA decreases, and the PSO, ICA, and proposed PSOICA meet the precision requirements. However, the results of the PSOICA include different solutions which always contain the optimal solution. That means that the PSOICA may present the best global searching ability among the four studied algorithms.

Table 5 is built to compare the global searching ability which is based on the data of 100 runnings for every algorithm.

Table 5. Comparing the results of four switching angles.

	Convergent Rate	One Solution	Two Solutions	Three Solutions
MGA	96%	60%	35%	1%
PSO	91%	91%	0	0
ICA	95%	32%	45%	18%
PSOICA	100%	5%	41%	54%

Compared to the proposed PSOICA, the conventional ICA has a lower convergent rate and a higher possibility of getting one solution. It shows that the proposed PSOICA enhances the global searching ability of the ICA. The PSOICA has a 54% chance of getting all three sets of solutions. The MGA barely obtains three solutions, and the PSO only has one solution in each calculation instant. Moreover, the convergent rate of PSOICA is also better than those of the MGA and PSO, which demonstrates the superiority of the PSOICA in global search.

According to the comprehensive comparative analysis above, it can be seen that the proposed PSOICA has advantages over the MGA, PSO, and ICA, regarding both global and local searching abilities.
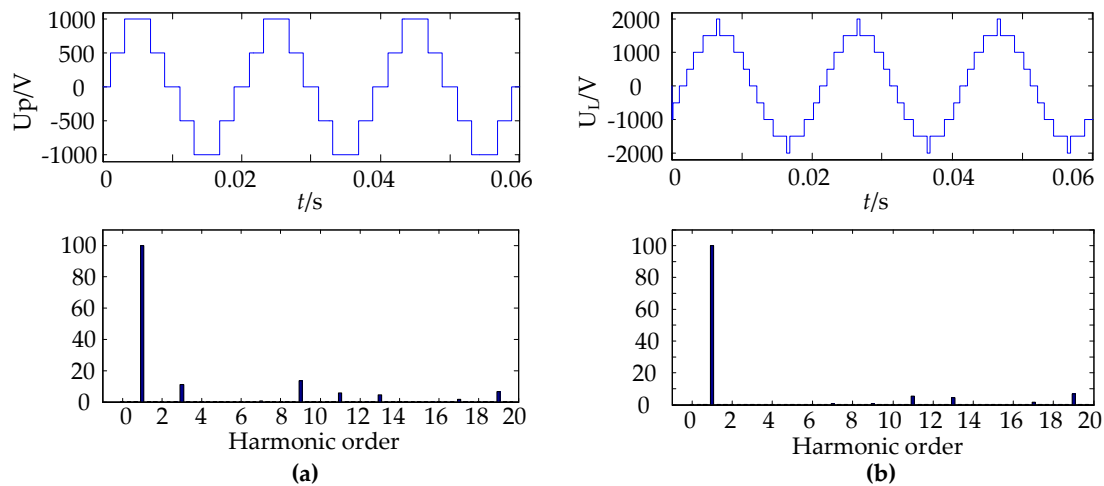
4. Simulation Analysis

To identify the correctness of solutions, we selected two different solutions, which are [20.3232, 56.3232] at 0.95 modulation index, and [62.4933, 81.5067] at 0.2 modulation index, and used Matlab/Simulink for simulation and harmonic analysis. The simulation conditions consisted of a fundamental output frequency of 50 Hz and a DC voltage of 1000 V.

In Figure 7, the phase voltage waveforms conform to the waveforms at low modulation shown in Figure 1a, and the amplitude matches the desired values exactly. A spectrum analysis shows that the selected 5th harmonic in phase voltage as well as the 5th and triple harmonics in line voltage are completely eliminated.

In Figure 8, the phase voltage waveforms are five-level, as shown in Figure 1b. The output voltages match the desired values exactly, and the selected 5th harmonic in phase voltage as well as the 5th and triple harmonics in line voltage are equal to zero. This verifies the correctness of switching angles and the effectiveness of the SHEPWM strategy.
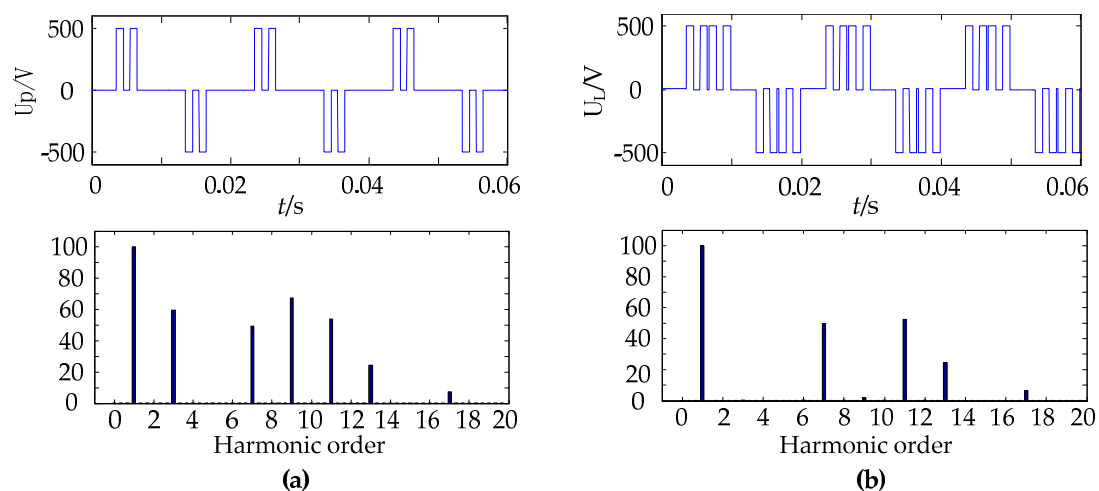

Figure 7. Simulation results with a modulation index of 0.2: (**a**) waveforms of phase voltage and its spectrum analysis; (**b**) waveforms of line voltage and its spectrum analysis.

Figure 8. Simulation and analysis with a 0.95 modulation index: (**a**) waveforms of phase voltage and its spectrum analysis; (**b**) waveforms of line voltage and its spectrum analysis.

Figure 9a displays the trends of two switching angles, and second solutions are found in the modulation index range of 0–0.605. The fact that the two solutions change regularly and work out at all modulation indexes is convenient for building a look-up table. Both these solutions meet various conditions of the five-level SHEPWM strategy and have different THDs. Figure 9b shows the THDs of the two solutions. For the first solutions, low and high waveforms correspond to the modulation index ranges 0–0.375 and 0.375–1.12, respectively. The second solutions merely work for waveforms of low modulation index, between 0 and 0.605. Taking THD into consideration, for the situation of two switching angles per quarter wave, we can conclude that, in the ranges of 0–0.551 and 0.605–1.12, the first solutions are better, whereas, in the remaining range, the second solutions are more suitable.
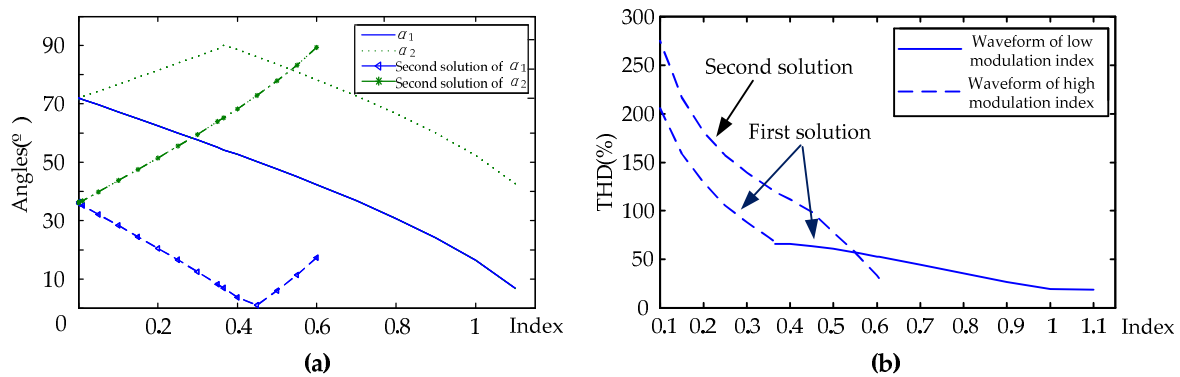
Figure 9. Trends of two switching angles and second solutions with the varying of the modulation index: (**a**) switching angles of the PSOICA; (**b**) THDs of the two different solutions.

5. Experimental Results

A downscaled three-phase NPC/H-Bridge five-level converter experimental prototype, shown in Figure 10, is set up to validate the proposed PSOICA. The power devices of the experimental prototype are insulated gate bipolar transistors (IGBT) modules (Infineon-BSM50GB120DLC). Meanwhile, a high-speed digital control platform based on the digital signal processor (DSP) (TI-TMS320F28335) and field programmable gate array (FPGA) (Xilinx-XC3S500E) is also adopted to implement the proposed PSOICA. The experimental conditions consist of the fundamental output frequency of 50 Hz and the DC voltage of 100 V.
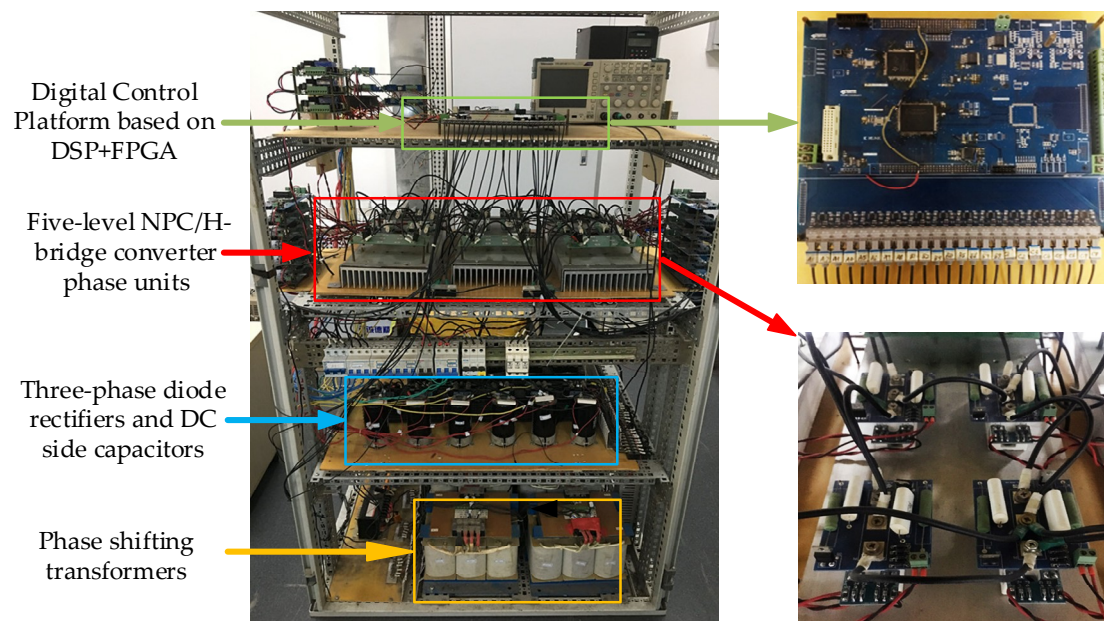
Figure 10. Three-phase neutral-point-clamped (NPC)/H-Bridge five-level converter experimental prototype.

Figure 11a shows the phase voltage and line voltage and their spectrum analysis under 0.2 modulation index. The waveforms are the same as those of the simulation results, and the selected 5th harmonic and triple harmonics are totally eliminated. Figure 11b exhibits the phase voltage and line voltage and their spectrum analysis under 0.95 modulation index. The phase voltage is five-level and the line voltage is nine-level, which are similar to the simulation results. Moreover, the selected harmonic and triple harmonics in line voltage are also removed. Hence, the analysis and simulation results are validated by these experimental results.
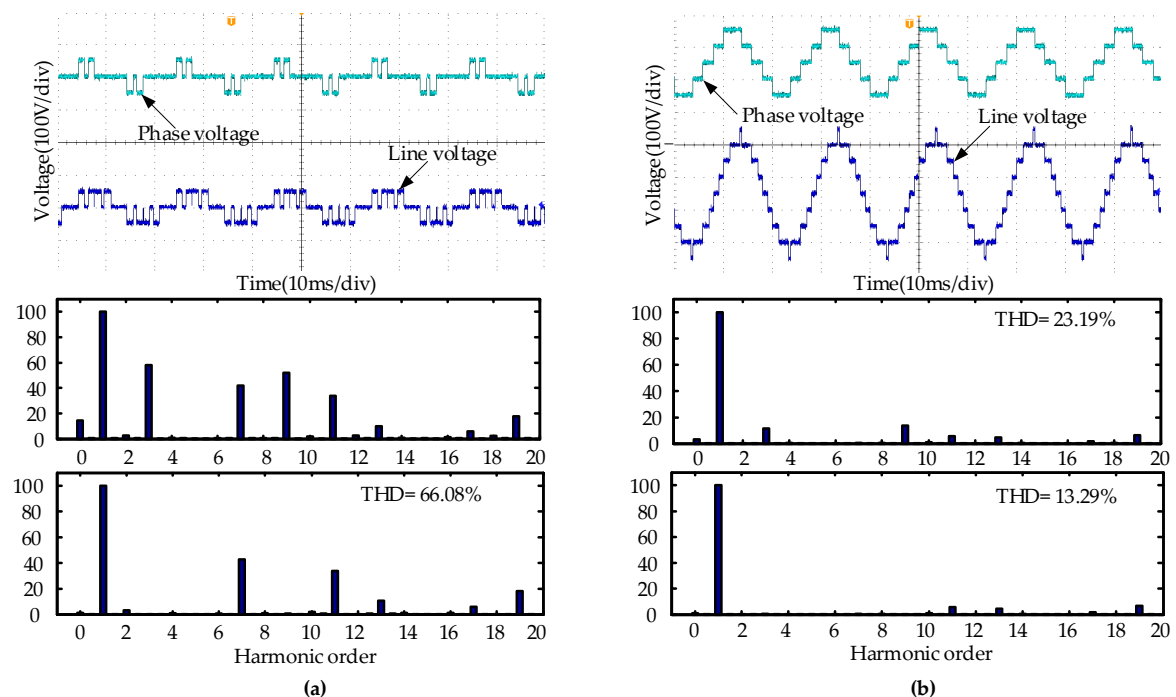
Figure 11. Experimental analysis of the waveforms: (**a**) waveforms of phase voltage and line voltage and their spectrum analysis under a modulation index of 0.2; (**b**) waveforms of phase voltage and line voltage and their spectrum analysis under a modulation index of 0.9.

As seen, a minor difference can be observed regarding the harmonic distribution characteristics between the simulation results (see Figures 7 and 8) and the experimental results. We think that this is mainly the result of two factors: one is the model difference between the simulation model and the actual experimental prototype, the other is the dead-time effect. As known, the IGBT model in the Matlab/Simulink is relatively ideal and can be regarded as a switch without the turn-on/turn-off time, so the dead-time is not set in the simulation research in this paper. However, for the experimental setup, the actual IGBT modules cannot switch as fast as the simulation models. Hence, for the experimental research described above, the dead-time was set to 4 μs in order to prevent a short circuit in each bridge arm. Considering that the SHEPWM is strongly associated with the switching time of the IGBTs, the above factors may cause the aforementioned minor difference.

6. Conclusions

In this paper, an improved ICA algorithm named PSOICA has been proposed for solving the multilevel SHEPWM. Two starting points were followed for designing the PSOICA: one was to increase the diversity and movements of the imperialists, the other was to enhance the ability to jump out of the local optimal. Hence, a novel type of particles, named independent countries, were brought into the conventional ICA to solve the nonlinear equations for the multilevel SHEPWM, especially for the situations with two and four switching angles per quarter wave. Compared to the existing MGA, PSO algorithm, and conventional ICA, the proposed PSOICA shows better performances both in global and local searching abilities, which verify the superiority of the proposed PSOICA. At the same time, the switching angles at different modulation indexes were calculated more accurately by the proposed PSOICA, which could help to obtain a more accurate modulating performance for various kinds of multilevel converters. Moreover, since a higher convergent rate can be obtained by the proposed algorithm, the execution time for solving the multilevel SHEPWM can also be reduced. Thus, the proposed PSOICA could provide a more appropriate solving approach for the SHEPWM with a high number of voltage levels.

References

1. Son, Y.; Kim, J. A novel phase current reconstruction method for a three-level neutral point clamped inverter (NPCI) with a neutral shunt resistor. *Energies* **2018**, *11*, 2616. [CrossRef]
2. Gong, Z.; Wu, X.; Dai, P.; Zhu, R. Modulated model predictive control for MMC-based active front-end rectifiers under unbalanced grid conditions. *IEEE Trans. Ind. Electron.* **2019**, *66*, 2398–2409. [CrossRef]
3. Rathore, R.; Holtz, H.; Boller, T. Generalized optimal pulse-width modulation of multilevel inverters for low-switching-frequency control of medium-voltage high-power industrial AC drives. *IEEE Trans. Ind. Electron.* **2013**, *60*, 4215–4224. [CrossRef]
4. Wang, Q.S.; Cheng, M.; Jiang, Y.L.; Zuo, W.J.; Buja, G. A simple active and reactive power control for applications of single-phase electric springs. *IEEE Trans. Ind. Electron.* **2018**, *65*, 6291–6300. [CrossRef]
5. Pouresmaeil, E.; Mehrasa, M.; Shokridehaki, M.A.; Rodrigues, E.M.G. Integration of renewable energy for the harmonic current and reactive power compensation. In Proceedings of the 2015 IEEE 5th International Conference on Power Engineering, Energy and Electrical Drives (POWERENG), Riga, Latvia, 11–13 May 2015; pp. 32–36.
6. Mehrasa, M.; Pouresmaeil, E.; Akorede, M.F. Multilevel converter control approach of active power filter for harmonics elimination on electric grids. *Energy* **2015**, *84*, 722–731. [CrossRef]

7. Mehrasa, M.; Pouresmaeil, E.; Zabihi, S.; Rodrigues, E.M.G. A control strategy for the stable operation of the shunt active power filters in power grids. *Energy* **2016**, *96*, 325–334. [CrossRef]

8. Srndovic, M.; Zhetessov, A.; Alizadeh, T.; Familiant, Y.L.; Grandi, G.; Ruderman, A. Simultaneous Selective Harmonic Elimination and THD Minimization for a Single-Phase Multilevel Inverter with Staircase Modulation. *IEEE Trans. Ind. Appl.* **2018**, *54*, 1532–1541. [CrossRef]

9. Zheng, C.H.; Zhang, B.; Qiu, D.Y. Solving switching angles for the inverter's selected harmonic elimination technique with walsh function. In Proceedings of the 2005 International Conference on Electrical Machines and Systems, Nanjing, China, 27–29 September 2005; pp. 1366–1370.

10. Dahidah, M.S.A.; Konstantinou, G.; Agelidis, V.G. A review of multilevel selective harmonic elimination PWM: Formulations, solving algorithms, implementation and applications. *IEEE Trans. Power Electron.* **2015**, *30*, 4091–4106. [CrossRef]

11. Chiasson, J.N.; Tolbert, L.M.; McKenzie, K.J.; Du, Z. Elimination of harmonics in a multilevel converter using the theory of symmetric polynomials and resultants. *IEEE Trans. Control Syst. Technol.* **2005**, *13*, 216–223. [CrossRef]

12. Jacob, T.; Suresh, L.P. A review paper on the elimination of harmonics in multilevel inverters using bioinspired algorithms. In Proceedings of the 2016 International Conference on Circuit, Power and Computing Technologies (ICCPCT), Nagercoil, India, 18–19 March 2016; pp. 1–8.

13. Guan, E.; Song, P.G.; Ye, M.Y.; Wu, B. Selective harmonic elimination techniques for multilevel cascaded H-bridge inverters. In Proceedings of the International Conference on Power Electronics and Drives Systems, Kuala Lumpur, Malaysia, 28 November–1 December 2005; pp. 1441–1446.

14. Aghdam, M.G.H.; Fathi, S.H.; Gharehpetian, G.B. Elimination of harmonics in a multi-level inverter with unequal DC sources using the homotopy algorithm. *IEEE Int. Symp. Ind. Electron.* **2007**, 578–583. [CrossRef]

15. Fei, W.M.; Du, X.L.; Wu, B. A Generalized half-wave symmetry SHE-PWM formulation for multilevel voltage inverters. *IEEE Trans. Ind. Electron.* **2010**, *57*, 3030–3038. [CrossRef]

16. Kumar, A.; Chatterjee, D.; Dsagupta, A. Harmonic mitigation of cascaded multilevel inverter with non-equal DC sources using hybrid newton raphson method. In Proceedings of the 2017 4th International Conference on Power, Control & Embedded Systems (ICPCES), Allahabad, India, 9–11 March 2017; pp. 1–5.

17. Yang, K.H.; Zhang, Q.; Yu, W.S.; Yuan, H.X. Selective harmonic elimination with groebner bases and symmetric polynomials. *IEEE Trans. Power Electron.* **2016**, *31*, 2742–2752. [CrossRef]

18. Ye, M.Y.; Zhou, Q.Q.; Hong, C.; Song, L. Multiple population genetic algorithm based on multi-band SHEPWM control technology for multi-level inverter. *Trans. China Electrontech. Soc.* **2015**, *30*, 111–119. [CrossRef]

19. Kumar, N.V.; Chinnaiyan, V.K.; Pradish, M.; Divekar, M.S. Enhanced power quality of MLI using PSO based selective harmonic elimination. In Proceedings of the 2015 International Conference on Green Computing and Internet of Things (ICGCIoT), Noida, India, 8–10 October 2015; pp. 42–47.

20. Kouzou, A.; Mahmoudi, M.O.; Boucherit, M.S. Application of SHE-PWM for seven-level inverter output voltage enhancement based on particle swarm optimization. In Proceedings of the 2010 7th International Multi- Conference on Systems, Signals and Devices, Amman, Jordan, 27–30 June 2010; pp. 1–6.

21. Atashpaz-Gargari, E.; Lucas, C. Imperialist competitive algorithm: An algorithm for optimization inspired by imperialistic competition. In Proceedings of the 2007 IEEE Congress on Evolutionary Computation, Singapore, 25–28 September 2007; pp. 4661–4667.

22. Mitras, B.A.; Sultan, J.A. A novel hybrid imperialist competitive algorithm for global optimization. *Aust. J. Basic Appl. Sci.* **2013**, *7*, 330–341.

23. Etesami, M.H.; Farokhnia, N.; Fathi, S.H. A method based on imperialist competitive algorithm (ICA), aiming to mitigate harmonics in multilevel inverters. In Proceedings of the 2011 2nd Power Electronics, Drive Systems and Technologies Conference, Tehran, Iran, 16–17 February 2011; pp. 32–37.

24. Cheng, Z.; Wu, B. A Novel Switching Sequence Design for five-level NPC/H-bridge inverters with improved output voltage spectrum and minimized device switching frequency. *IEEE Trans. Power Electron.* **2007**, *22*, 2138–2145. [CrossRef]

25. Chang, H.; Wei, R.; Ge, Q.; Wang, X.; Zhu, H. Comparison of SVPWM for five level NPC/H-Bridge inverter and traditional five level NPC inverter based on line-voltage coordinate system. In Proceedings of the 2015 18th International Conference on Electrical Machines and Systems (ICEMS), Pattaya, Thailand, 25–28 October 2015; pp. 574–577.

26. Taleb, R.; Helaimi, M.; Benyoucef, D.; Boudjema, Z. A comparative analysis of multicarrier SPWM strategies for five-level flying capacitor inverter. In Proceedings of the 2016 8th International Conference on Modelling, Identification and Control (ICMIC), Algiers, Algeria, 15–17 November 2016; pp. 608–611.

27. Mehrasa, M.; Pouresmaeil, E.; Akorede, M.F.; Zabihi, S.; Catalao, J.P.S. Function-based modulation control for modular multilevel converters under varying loading and parameters conditions. *IET Gener. Transm. Distrib.* **2017**, *11*, 3222–3230. [CrossRef]

28. Ayyappa, P.N.V.S.; Srinivas, C.; Singh, T.R.S. A novel way to deal with harmonic elimination in multi-level CHB inverter using without filtering technique. In Proceedings of the 2017 International conference of Electronics, Communication and Aerospace Technology (ICECA), Coimbatore, India, 20–22 April 2017; pp. 62–67.

29. Fei, W.; Wu, B.; Wu, Q. A novel SHE-PWM method for five level voltage inverters with quarter-wave symmetry. In Proceedings of the 2009 Canadian Conference on Electrical and Computer Engineering, St. John's, NL, Canada, 3–6 May 2009; pp. 1034–1038.

30. Dahidah, M.S.A.; Agelidis, V.G.; Rao, M.V. On abolishing symmetry requirements in the formulation of a five-level selective harmonic elimination pulse-width modulation technique. *IEEE Trans. Power Electron.* **2006**, *21*, 1833–1837. [CrossRef]